

MAGIC NUCLEI MAGNETODYNAMICS IN MAGNETAR CRUSTS

V. N. Kondratyev, I. M. Kadenko

Taras Shevchenko National University, Kyiv, Ukraine

The magnetodynamics of inhomogeneous nuclear matter relevant for neutron star crust is considered. The quantization effects are demonstrated to result in sharp abrupt magnetic field dependence of nuclide magnetic moments. Accounting for inter-nuclide magnetic coupling we show that such anomalies give rise to erratic jumps in magnetotransport of neutron star crusts. The properties of such a noise are favorably compared with burst statistics of Soft Gamma Repeaters.

1. Introduction. Soft Gamma Repeaters and Anomalous X-ray Pulsars as Magnetars

Ultramagnetized astrophysical objects ('magnetars') have been invoked to interpret several astronomical phenomena associated with an activity of Soft Gamma Repeaters (SGRs) and Anomalous X-ray Pulsars (AXPs). Such high-energy transient astrophysical sources display also persistent X-ray luminosity $L_X \sim 10^{34.5} - 10^{36}$ erg/s, which are considerably smaller than the Eddington limit $L_{Edd} \approx 10^{38} (M_{NS} / M_{\odot})$ erg/s (see, e.g., [1]). However, the applicability of an accretion model to these neutron stars (NSs) meets serious difficulties [2]. The observed periods and period derivatives of SGR 1806-20 [3], SGR 1900+14 [4], AXPs 1E 1841+045 [5], and 1E 2259+586 [6] yield large values, up to tenths of *tera-tesla*, for the strength of dipole-surface-field components when assuming a magnetic-braking spin-down mechanism. Many observed properties of SGRs and AXPs strongly support the magnetar concept suggesting an ultra-magnetized stellar media with magnetic induction strength H up to hundreds of *tera-tesla*. Such a magnetization can be understood, e.g., as an effect of the magneto-rotational instabilities and/or "dynamo action" processes which might operate in fast rotating stars [7], or spontaneous magnetization of hadron liquid due to ferromagnetic exchange coupling [8].

It is worthy noticing here that the surface magnetic field does not necessarily reflect the strength of interior fields. For instance, toroidal fields below the Sun surface are stronger than average surface dipole fields [9] by at least a factor $10^2 - 10^4$, an excess corresponding to an interior field strength $H \sim 0.1 - 100$ TeraT in NSs. Indeed, the multip peaked pulse profile in the tail of the 1998 August 27 flare and following August 29 event (afterglow) of SGR 1900+14 gives an evidence [10] for essentially multipolar geometry of surface fields with high order multipoles plausibly stronger than the respective dipole component $H_d \sim 0.1$ TeraT. The energy associated with such super-strong fields dominates the star free energy, exceeds the rotational one and powers the magnetar emission.

Apart from mentioned above giant flares of a superhigh intensity $L_X \sim 10^{44.5}$ ergs these sources more generally emit the short (~ 0.1 s) outbursts with super-Eddington luminosity, i.e., $\sim 10^3 - 10^4 L_{Edd}$. Such burst emissions tend to concentrate into short intervals (weeks to months) of intense activity separated by relatively long (years) quasi-regular quiescent periods ([3], see also Eq. (7) of sect. 4 and discussion therein).

Many properties of SGR activity are well explained within 'magnetar' concept assuming that the emission of SGR bursts originates from the crust dynamics driven by the magnetic field, see [10, 11] and refs. therein. However, quasiperiodicities in SGR active phases in conjunction with rather stable (without noticeable spin-up glitches) spinning down provide arguments opposing the star-quake triggering mechanism of SGR bursts. Some alternative models have considered exotic processes, like collisions of a strange star with asteroids [12, 13], or effects of boson condensate in superconducting core [14].

As is argued in recent papers [11] these properties of the bursts activity can be understood within the magnetar concept as well and they are consistent with burst triggering mechanism due to a release of magnetic energy stored in NS crusts. The periods of intense activity are related to the step-like anomalies in magnetic field dependence of the magnetic moments of crust nuclides due to quantization. At such conditions the demagnetization proceeds as erratic jumps associated with crust magnetic avalanches, similar to the Barkhausen effect (see, e.g., [15] and sect. 2), and causes sharp energy release to the magnetosphere. Significant difference from the Barkhausen noise is the strongly magnetized system far from conditions of magnetization reversal.

In this contribution we further demonstrate that discontinuities in crust magnetodynamics due to quantization of spatial motion naturally arises in the inhomogeneous crusty nuclear matter suggested by numerous theoretical studies (cf. [11, 16 - 19] and refs. therein) at the density D less than the saturation density

D_s . The properties of nuclear matter at such transitional densities are particularly important, indeed, with respect to the studies of the Equation of State. As is shown recently [11, 16 - 19] the structure of NS envelopes and the nuclide composition can depend on the magnetic field. Such an effect originates from the modification of shell-oscillations in the nuclear level density (and, consequently, the masses of atomic nuclei) under an influence of magnetic fields, similarly to atomic clusters and quantum dots (cf. [20 - 23] and refs. therein). As is demonstrated accounting for nuclear moment jumps at crust magnetodynamics yields accurate quantitative description of the SGR burst statistics during the active period which displays features of self-organized criticality, e.g., power law dependence of number of events on the intensity, lognormal distribution of waiting times between the bursts [24 - 26].

2. Magnetization of atomic nuclei

As is indicated above the NS outer crusts can be viewed as polycrystalline hetero-structure composed from well-separated atomic nuclei. The quantization of nucleon spatial motion represents specific feature for atomic nuclei, which gives rise to the sharp step-like jumps of the magnetic response in varying magnetic fields due to the Zeeman splitting of the energy levels. We recall here, that within the Hartree self-consistent mean field approach the single-particle energy levels determine the shell effects. Applications of the Nilsson model (see, e.g., [27]) are very successful in understanding of many properties of stable nuclei in the region of average mass numbers $A \sim 10 - 100$. Employing such a model one incorporates the harmonic oscillator (HO) spectrum of a frequency $\omega_0 \approx 41/A^{1/3}$ MeV and accounts for the spin-orbit splitting of energy levels with a gap $\eta_{so} \approx 0.12$ (in units ω_0).

The contribution of neutrons to the magnetic response of a nucleus is exhibited by the spin magnetization of Pauli type. Such reactivity originates from an interaction of a field and the spin-magnetic moment. Energy levels of neutrons corresponding to a spin projection m_n on a field vector are shifted linearly on a value $\Delta = m_n g_n \omega_L$ with the neutron g-factor g_n , Larmour frequency $\omega_L = \mu_N H$ and nucleon magneton μ_N . It results in a phase shift of shell oscillations in binding energy versus neutron number [16 - 19]. Respectively, the neutron component $M_n = (N_\uparrow - N_\downarrow) g_n \mu_N / 2$ in total magnetic moment M of nucleus is determined by an excess $N = N_\uparrow - N_\downarrow$ of majority-spin N_\uparrow over minority-spin N_\downarrow neutrons. It gives rise to step-wise anomalies in field dependence of nuclear magnetization at the conditions of level crossing, see Fig. 1.

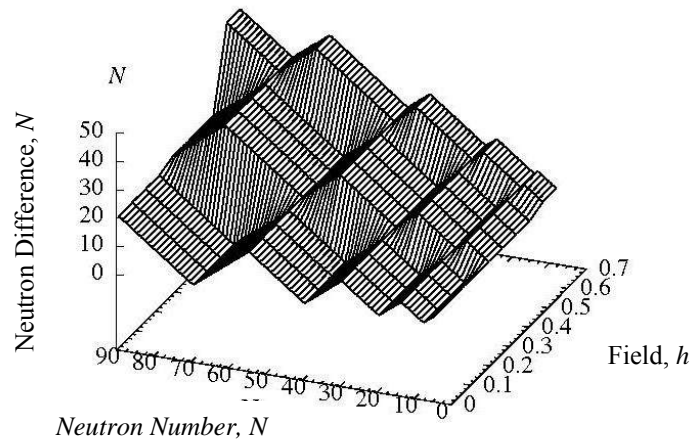


Fig. 1. The difference N of majority-spin N_\uparrow and minority-spin N_\downarrow neutrons versus the neutron number and the magnetic field strength $h = \omega_L / \omega_0$ as predicted by spherical HO potential.

The physical origin of such a jump of nuclear magnetic moment can be rather clearly understood within the following qualitative picture applied for the spherical HO potential. Let us consider a magic nucleus with a filled neutron shell, i.e. the number of neutrons on the highest occupied shell corresponds to the degeneracy number. For a case of zero spin-orbit coupling such a nucleus could have, e.g., 40 neutrons ($N = 40$) when the shell with the principal quantum number $n = 3$ is just filled. At zero magnetic field such a magic nucleus has zero magnetic moment and corresponds to a negative minimum of the shell-correction energy (see [27]). The magnetic field shifts majority- and minority-spin neutron levels down and up, respectively (see [11, 16, 17]). At the field strength corresponding to the energy shift on a half of HO frequency (i.e. $h = |0.5/g_n|$) the

majority- and minority-spin energy levels cross. Therefore, 20 spin-up neutrons of $n = 3$ shell (at $h < |0.5/g_n|$) are rearranged to occupy the spin-down $n = 4$ shell. Consequently, the magnetic moment of such a nucleus is changed step-wise at the level crossing. We recall here that the neutron magnetization corresponds to the spin alignment reversed to the magnetic field vector due to the negatively defined neutron gyromagnetic ratio. Therefore, in the magnetic field the relative number of spin-down neutrons exceeds the number of spin-up neutrons. However, the actual balance between the minority- and majority-spin neutrons is rather sensitive to the shell structure.

Magnetic response of protons is represented by a superposition of field interaction with spin and orbital magnetic moments [11, 16 - 19] with frequenter jumps as compared to the neutron response.

3. Modeling the Magnetodynamics of Crusty Nuclear Matter

As is pointed out in sect. 2 the quantization of spatial nucleon motion gives rise to the step-like jumps of the magnetic response in varying magnetic fields. In particular outer crust nuclides display such an anomaly at the crossing of nuclear levels. In this section we demonstrate that these properties result in the noise during the crust demagnetization. As a consequence, the time evolution of magnetic fields experiences erratic jumps leading to a sharp energy release to the magnetosphere of the magnetic energy stored in, e.g., the nuclear degrees of freedom of NS crusts. Therefore, within present picture the mechanism of SGR burst emission by a magnetar is similar to the generation of a noise in the loudspeaker by the coil of a wire surrounding a ferromagnet and being put under the conditions of magnetization reversal by external varying magnetic field, i.e. the magnetic Barkhausen emission (see, e.g., [15]). Because of the domain structure the dynamics of magnetic field exhibits some sharp changes with time. Such a jump induces a current in a wire. The energy released to the coil-wire is determined by the magnetic induction $B = H_{ext} + P_F$ with applied field H_{ext} , and magnetization of a ferromagnetic P_F as well as respective volume V_{magn} and can be estimated to be

$$E \approx B \cdot P \cdot V_{magn} \quad . \quad (1)$$

The analogy can be seen between the crust and ferromagnetic as well as between the magnetosphere and the coil-wire. We note that 'magnetar' related processes considered here correspond to ultramagnetized media and energy scale larger by about 30 orders of magnitude. Furthermore, the sharp change of crust magnetization originates from step-wise behavior of the nuclide magnetic moments rather than from magnetization reversal.

3.1. Magnetic Coupling, Disorder and Fluctuations in Outer Crusts

In this section we quantify some observables related to crust magnetodynamics on the basis of phenomenological and theoretical analysis of observations. The induced magnetic moment of nuclides contributes to the magnetization of NS crusts. For aligned moments the respective component in magnetic induction is given by

$$P = M_N / V_{WS} \approx (M_N / \mu_N A)(D_b / D_s) \cdot 0.1 \text{ TeraT}, \quad (2)$$

where the nuclear magnetic moment $M_N = M_n + M_p$ is represented as a sum of neutron M_n and proton M_p contributions, see sect. 2, while an average density of bound nucleons $D_{Nb} = A/V_{WS}$ is related to the Wigner-Seitz volume V_{WS} and can be evaluated as several tenths of normal nuclear density D_s .

We consider the outer crusts as a polycrystalline hetero-structure with nuclei arranged in a closed packed (plausibly bcc) lattice and assume the dipolar interaction between magnetic moments M_i and M_j of nuclei i and j . Such a system shows the ferromagnetic ordering (see e.g. [11]) with the easiest magnetization axis $\{100\}$. The coupling constant J and an anisotropy energy density K can be estimated from the lattice parameters as

$$J_d \approx M_i M_j / a^3 \approx 0.01 \text{ MeV}, \quad K_d \approx 0.1 J_d / V \approx 10^{26} \text{ ergs/cm}^3, \quad (3)$$

where $a \sim 10^{1.5}$ fm stands for the lattice constant. The coupling strength J_d corresponds to an effective magnetizing field $P = J_d / M \approx 10^{-2.5}$ TeraT, cf. Eq. (2).

Another essential feature of realistic systems is associated with fluctuations and randomness: dirt. Usually the system contains inhomogeneity and disorder in the form of defects, grain boundaries, impurities, leading

to random crystalline anisotropies, and varying interaction strengths in the crystalline structure. Apart from such static spatial fluctuations h_{st} we bear in mind dynamical components h_d due to inexactness of the model description (see sect. 4). Simple way to implement a certain kind of uncorrelated quenched disorder as well as fluctuations is provided by identifying such effects with uncorrelated random fields h_i associated with each site of the lattice, and distributed according the gaussian distribution function

$$W(h) = \exp\{-h^2 / R^2\} / R\sqrt{\pi} \quad (4)$$

as one expects from the central limit (or normal convergence) theorem. We refer to the width R as for the disorder. In the order of magnitude this quantity can be evaluated as an effective magnetizing field $R \sim P \sim 0.01 \text{ TeraT}$, cf. Eqs. (2) and (3).

It is worthy to notice here that such a value of R is smaller than an expectation for the inter-jump magnetic field spacing β_{jmp} . Average value of the spacing is defined by the field interval between the successive jumps b_{n-1} and b_n , i.e. $\beta_{jmp} = \langle H_n - H_{n-1} \rangle_n$, where $\langle \bullet \bullet \rangle_n$ denotes an averaging over level crossing n . To calculate the field spacing we note that two levels with energy difference $\delta\mathcal{E}$ cross in the field interval $\delta H = \delta\mathcal{E} \cdot (d(\delta\mathcal{E})/dH)^{-1}$. For neutrons the change rate of the energy difference is given by $(d(\delta\mathcal{E})/dH)_n \approx g_n \mu_N \approx 0.1 \text{ MeV/TeraT}$. The inter-jump field spacing can be, therefore, evaluated from the total nuclear level spacing $\delta\mathcal{E}$ as $\beta_{jmp} = (d(\delta\mathcal{E})/dH)^{-1} \delta\mathcal{E} = (d(\delta\mathcal{E})/dH)^{-1} / W$. In the second equality of this expression we take into account that the level spacing is given as an inverted total nuclear level density $\delta\mathcal{E} = W^{-1}$ [27]. Since the case of shifted energy levels in the magnetic field corresponds to an excited nucleus, the field spacing is estimated, $\beta_{jmp} \sim 10^{-2.5} \text{ TeraT}$, to be larger as compared to disorder effects.

3.2. The Randomly Jumping Interacting Moments Model as an Extension of the Ising Model

To model the long-range, far from equilibrium, collective behavior mentioned in the beginning of the section (sect. 3), we define the crusts as a collection of Π domains on a hypercubic lattice [11, 20 - 23] with magnetic moments per nucleus m_i which changes step-wise as a function of local magnetic fields b , $m_i = \mu_N \sum_n \nu_n \theta(b - b_n)$ with jumps of a height ν_n at field strengths b_n corresponding to level crossings. Here the step-function $\theta(x \leq 0) = 0$ and $\theta(x > 0) = 1$.

According to an analysis of previous sect. 3.1 the coupling between nearest neighbor (nn) domain-moments is ferromagnetic of a strength J_{ij} , and they interact with a uniform magnetic field H directed along the moments. Then introducing the total magnetization (below is also referred to as a mean-field) $P = \Pi^{-1} \sum_i m_i$ we express the Hamiltonian of the outer crust domains as

$$H_1 = - \sum_{i,j \subset nn} J_{ij} m_i m_j - HP, \quad (5)$$

where it is understood that the sum runs over nearest neighbor pairs of moments on the sites i and j .

When moments m_i are allowed for two values ± 1 , the Hamiltonian Eq. (5) represents the Ising model which reliably describes the effects of spontaneous magnetization as well as hysteresis and discontinuities in reversing the magnetization (i.e. magnetization curve). As outlined below in this section within the dynamical picture such effects can be interpreted as magnetic avalanches in the system.

As is pointed out in sect. 3.1 in order to simulate realistic systems it is required to incorporate in the Hamiltonian Eq. (5) fluctuating fields (see Eq. (4) and discussion therein). Such fluctuations can prevent the spontaneous magnetization of entire system by keeping it on a metastable state. As a consequence, the magnetization curve is modified, i.e. not all the domain-moments jump at the same value of the external magnetic field. Instead, they jump in avalanches of various sizes that can be broken up or stopped by strongly "pinned" magnetic moments or clusters of previously jumped moments. When the disorder in the crust is small, the picture is qualitatively similar to the pure case of the Ising model. One would expect the predominant macroscopic discontinuity at critical field with a few small precursors in the vicinity. Large disorders, as compared to the coupling strength J , can wash out the sharp transition and result in smooth and almost macroscopically continuous magnetization curve. Applying random fields the Hamiltonian is then given by $H = H_1 + \sum_i h_i m_i$. For analytic calculations and simulations we set the interaction between the

moments to be independent of the moments and equal to J for the nearest neighbors $J_{ij} = J$ and zero otherwise. Then the crust magnetodynamics is determined by the magnetic moment m_i jumps which occur when the difference between its local effective field b_i :

$$b_i = J \sum_{j \subset nn} m_j + H + h_i \quad (6)$$

and some of the quantities b_n , i.e. the value $\Delta b = b_i - b_n$ changes sign.

At the condition $b_{n+1} - b_n \gg \Delta b \gg R$ almost all the moments equal to the value $\zeta_n = \sum_{i=-\infty}^n v_i$ and point along the direction of a field \mathbf{H} (i.e. $m_i = \zeta_n$ for all i). As the field adiabatically decreases the moments progressively jump to $\zeta_{n-1}, \zeta_{n-2} \dots$. Because of the nearest neighbor interaction, the jumped moment can result in the jump of a neighbor which in turn might lead to the reducing moment of another neighbor, and so on, generating thereby an avalanche of moment jumps. The adiabatically changing field $H(t)$ implies that the external field is kept constant during each avalanche, while the magnetization varies according to the definition of the mean-field, see Eq. (5) and discussion therein.

At large disorders corresponding to the wide distribution of random fields the magnetic moments tend to jump independently of each other. Small avalanches give rise to the smooth (on a macroscopic scale) magnetization curve. On the other hand, small disorder implies a narrow random field distribution, which allows for large avalanches. This leads to noticeable discontinuities in the magnetization curves, similarly to what is found for the Ising model at zero temperature. At transitional values of the parameters $R = R_c$ and $H = H_c$ the system shows critical scaling behavior and the widest distribution of the avalanche sizes [11, 22, 23]. We refer for such a model as randomly jumping interacting moments (RJIM) model.

4. RJIM model Implications in SGR-Burst Activity

As is shown in sect. 3 the NS crust magnetotransport exhibits irregular jumps, when magnetic fields match the vicinity of step-wise anomalies of nuclide magnetic moments. Such an epoch of NSs is represented schematically in Fig. 2. As shown in the inset of the right panel of Fig. 2 the RJIM model confirms very short periods for the burst activity with rather small time intervals between the bursts which are associated with step-like change of the crust magnetic field. Such sharp decrease of the magnetization is caused by avalanches of the magnetic moment jumps due to ferromagnetic coupling between nuclides. The proportional to the avalanche size excess of magnetic energy is released to the magnetosphere. Assuming the

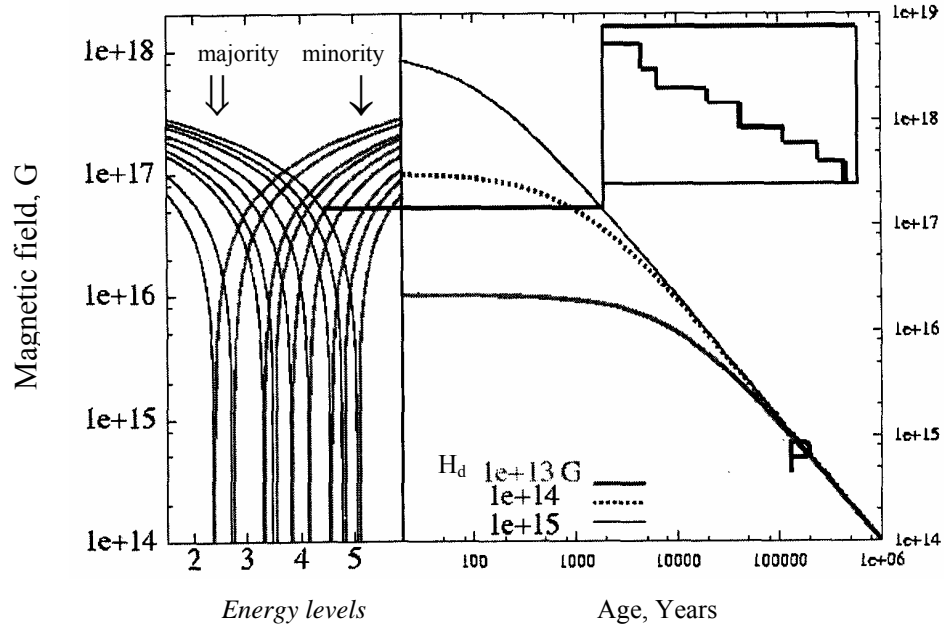


Fig. 2. Schematic view of neutron star crust magnetotransport. The left panel shows the magnetic field dependence of neutron majority- and minority-spin energy levels for NM, decreasing and increasing with the field, respectively. The right panel represents the time evolution of overall magnetic field with an inset displaying the magnetodynamics during the active bursting period. The respective level crossing (see text) is indicated by horizontal line intersecting the left and right panels.

field strength of a couple of *TeraTesla* in the outer crust of a linear size $l_{\text{crust}} \sim 100 \text{ m}$ and employing an estimate Eq. (2) the energy upper limit is evaluated $E_{\text{max}} \sim HP_{\text{Ncrust}} l_{\text{crust}}^3 \approx 10^{42} \text{ ergs}$ to be in a good agreement with SGR-burst observations, the detailed comparison is given in sect. 4.1. This energy is larger by about 30 orders of magnitude as compared to the case of magnetic Barkhausen emission (see Eq. (1) and discussion therein). When the de-magnetization jumps involve the inner crust as well, the linear size is an order of magnitude larger and the energy release extends up to $10^{45} \text{ -- } 10^{46} \text{ ergs}$ and even beyond, a value corresponding to giant flare events.

The typical time for the energy release is associated with the spanning time of the crust linear size, $\tau_{\text{av}} \approx l_{\text{crust}} / c_m$. The speed of an avalanche propagation c_m is determined by the relaxation time τ_N of nuclear reconfiguration associated with magnetic response. Applying familiar value $\tau_N \approx 10^{-20.5} \text{ s}$ we find for the speed $c_m \approx l_{\text{crust}} / \tau_N \approx 10^8 \text{ cm/s}$. The corresponding estimate for spanning time $\tau_{\text{av}} \approx 10^{-1} \text{ ms}$ is in a good agreement with rising time of SGR-bursts [3, 4]. In the reminder of this section we analyze statistical properties of SGR-burst activity, common for various pulsars.

4.1. The SGR-Burst Statistics

Fig. 3 represents the cumulative distributions of detected fluence, i.e. the burst number with a fluence exceeding certain value, as observed by different missions, sensitive to individual regions of emitted energy. The observed distributions are well fitted by the power law dependence. Relevant exponents range from 0.47 to 0.97. The cumulative avalanche size distribution in the vicinity of the critical point is compared in Fig. 4 with the normalized cumulative fluence distribution. In the energy range exceeding 5 periods the observations by various missions are in a good agreement with simulations when accounting for the scale of the energy release given above in sect. 4, remoteness of ten kpc, and nearly isotropic emission of such objects. Some difference between the data and simulations at the regions corresponding to lower limits of the energies of detectors could be due to reducing detector efficiencies. The obtained event number dependence is well fitted by the power law with an exponent 0.67, which corresponds to the value 1.67 for the differential distribution and provides a signal of self-organized criticality in the burst statistics.

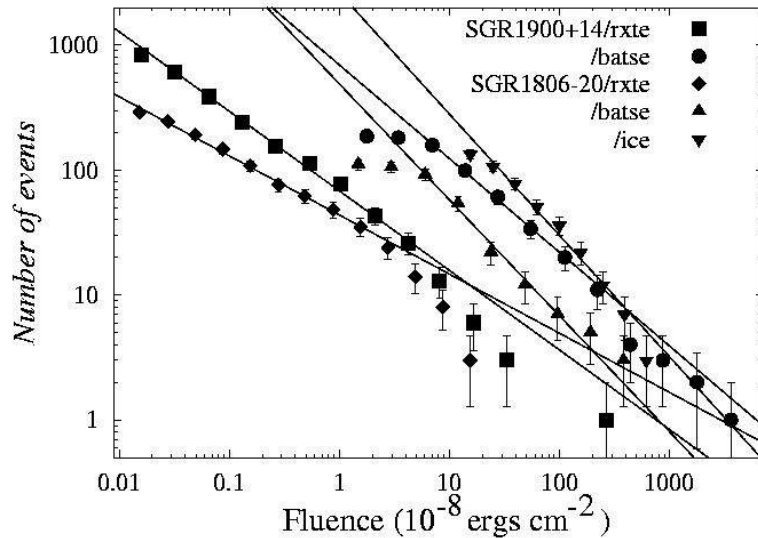


Fig. 3. Cumulative fluence distribution of SGR-bursts as observed by various missions for SGR 1900+14 bursts from [25] are shown by squares (Rossi X-ray Timing Explorer - RXTE) and circles (Bursts And Transient Source Experiment - BATSE). RXTE (diamonds), BATSE (up-triangles), and ICE (down-triangles) data for SGR 1806-20 are from [26].

For the case of a constant change rate \dot{B} of the magnetic field the inter-avalanche field interval is proportional to the time interval (i.e. waiting time) between the induced bursts. Taking the respective normalized values, i.e. inter-burst time and inter-avalanche field, we compare the theoretical predictions with observations in Fig. 5. The theoretical results are shown for the events, i.e. avalanches, covering the entire range of intensities of Fig. 4, while the observations are only for bursts registered by RXTE/PCA detector set. As we have seen, however, from analysis of simulation data, the applications of constraints or limits on the avalanche sizes influences considerably the position of the distribution maximum, while the width is only slightly affected.

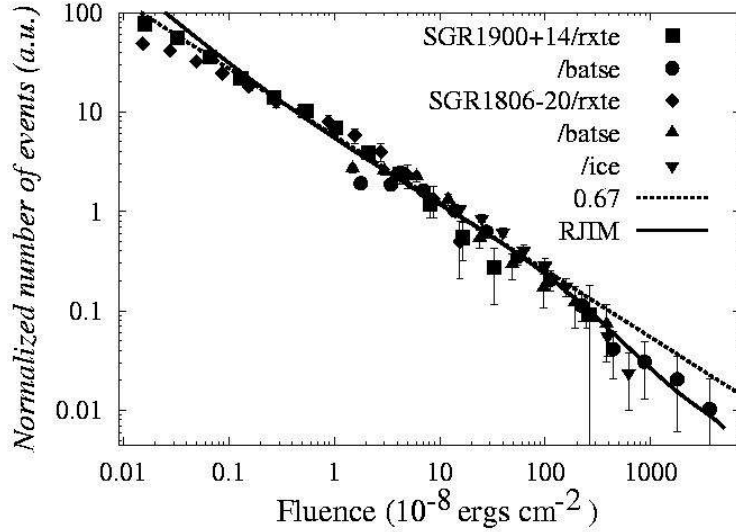


Fig. 4. Normalized cumulative fluence distributions of SGR-bursts. The results of the RXTE and BATSE observations for SGR 1900+14 from [25] are shown by squares and circles, respectively. RXTE (diamonds), BATSE (up-triangles), and ICE (down-triangles) data for SGR 1806-20 are from [26] are compared with the avalanche size distribution from RJIM for the cubic lattice of a size $(150)^3$ represented by the solid line. The dashed line denotes the power law distribution.

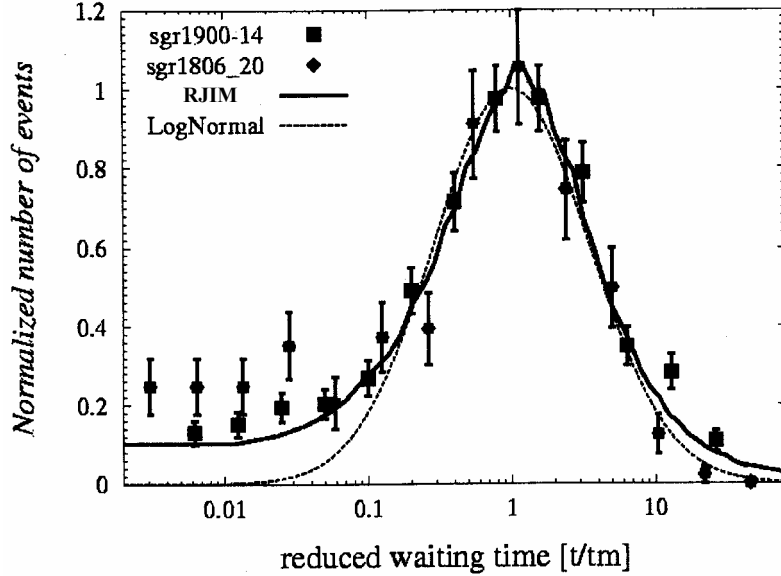


Fig. 5. The reduced waiting time distribution between the successive RXTE/PCA bursts from SGR 1900+14 (squares) [25] and SGR 1806-20 (diamonds) [26] are compared with the waiting time distribution between avalanches (solid curve). The dashed line represents the fit to the lognormal distribution of the width 3.6.

As seen in Fig. 5 for different SGRs the waiting time distributions as a function of the reduced time, i.e. the time normalized at the maximum, obey universal function. The data are well reproduced by simulations and fitted at a maximum by the lognormal function $LN(t) = \frac{\theta(t)}{\sqrt{2\pi t \ln(\sigma)}} \exp\left\{-\frac{(\ln(t/t_m))^2}{(\ln(\sigma))^2}\right\}$ with a width $\sigma \approx 3.6$. Such a property points out the single time scale for SGR-burst triggering processes. Within RJIM model such a time-scale is determined by the ratio of the disorder parameter R and the field change rate $\tau = R/\dot{B}$. Therefore, the scaling with respective time leads to an universal function. It is worthy to point out here the difference in the field change rate during quiescent and active phases.

4.2. The Periods of Burst Active Phases

According to presented RJIM model the star enters the phase of intensified burst activity when the magnetic field approaches critical values. An expectation time T_s for an inactive evolution is then determined by the ratio of the spacing β_{jmp} of magnetic moment jump anomalies (see sect. 3.1) and the rate \dot{B} of overall

field change, $T_s \approx \beta_{\text{jmp}} / \dot{B}$. Since the magnetic free energy $F_B \sim B^2$ dominates and powers the emission we find $\dot{B} \sim -L_p / B$. Using the familiar [1] relation for persistent luminosity $L_p \sim B_p^2$ and assuming the proportionality of the crust field to the field on star magnetic poles $B \sim B_p$, we obtain

$$T_s^2 L_p = \text{const} \quad (7)$$

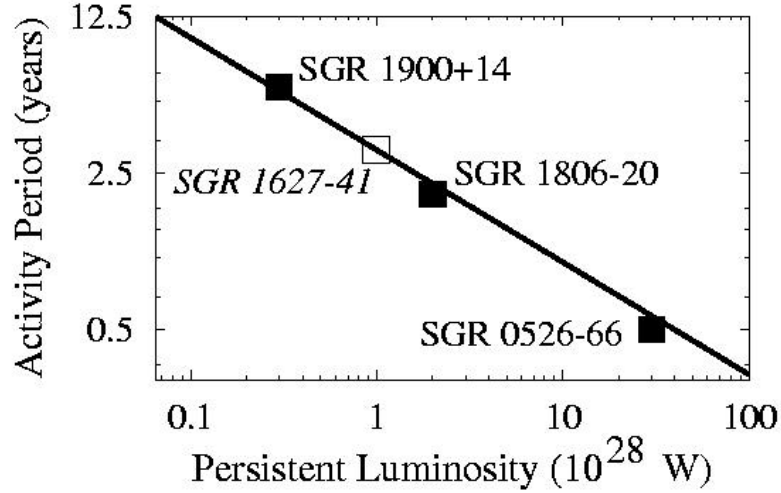


Fig. 6. Period of SGR's active phases versus the persistent luminosity. The observational data are from [11]. The solid line indicates the systematics with $\{\text{const} = 10^{43.5} \text{ erg s}\}$ (see text).

As illustrated in Fig. 6 SGR's observables follow rather well the systematics given by Eq. (7). We note, however, that fluctuations of level spacing and, corresponding, intervals of magnetic moment jumps give significant variations of activity periods, like in case of SGR 1900+14.

5. Conclusions

We have considered the magnetodynamics of NS crusts corresponding to the nuclear densities below the neutron drip line and being plausibly composed of well-separated magic nuclei, cf. [1, 11]. As is demonstrated the nuclear magnetization displays the sharp abrupt field dependence due to quantization of three-dimensionally confined spatial motion of nucleons. The Pauli-type paramagnetic response of neutrons results in discontinuities of magnetic moment arising almost periodically at the crossings of majority- and minority-spin energy levels. The proton contribution to the magnetization displays frequenter jumps of nuclear moments because of the relationship between the spin- and Landau-orbital-magnetism.

As is shown for NS crusts such jump anomalies of magnetic moments in conjunction with ferromagnetic inter-nuclide coupling give rise to jerky magnetodynamics with erratic sharp step-wise discontinuities in the crust (de)magnetization process due to avalanche propagation. As a consequence, sudden energy releases to the magnetosphere lead to SGR-bursts [11].

For the description of such noisy collective magnetodynamics of NS crusts we develop the Randomly Jumping Interacting Moments (RJIM) model accounting for quantum fluctuations due to the discrete level structure, inter-nuclide coupling, and disorder. The comparison of model predictions with observational data allows, therefore, quantifying crust properties. The magnetic equation of state identifies [11] conditions corresponding to the occurrence of self-organized criticality when the system exhibits universal scaling behavior and displays the widest distribution of discontinuity amplitudes.

As is shown the predicted by RJIM model scaling properties for, e.g., the burst intensity and waiting time distributions, are in a good agreement with SGR observations supporting thereby the credibility of RJIM model. As is implied within considered treatment the specific feature classifying SGRs is plausibly represented by the crust ultra-strong toroidal and multipolar magnetic field components matching the strength region of important quantization effects in nuclide magnetization. For outer crusts such fields approach *tera-tesla*, while weaker fields are expected for neutron-rich nuclides of inner crusts [11]. Further implications of the proposed magnetic emission mechanism in the analysis of SGR activity can provide better understanding of NS crust, in particular, strengths and evolution of magnetic fields. We note, however,

an importance of detail analysis of electronic excitations accompanying the nuclear dynamics, cf. [28, 29].

This work is supported in part by VIRGO observatory at Physical Faculty of Taras Shevchenko National University. The authors are indebted to B. Hnatyk and D. Jakubovskiy for valuable discussions, constructive comments and interesting suggestions.

REFERENCES

1. *Shapiro S.L., Teukolsky S.A.* Black Holes, White Dwarfs and Neutron Stars. - NY: Willey, 1983.
2. *Li X. D., Wang Z. R.* Spin-down rates of anomalous X-ray pulsars // *Astrophys. J. Lett.* - 2000. - Vol. 544. - P. L49.
3. *Kouveliotou C., Dieters S., Strohmayer T. et al.* An X-ray pulsar with a superstrong magnetic field in the soft gamma-ray repeater SGR 1806-20. - *Nature (London)*. - 1998. - Vol. 393. - P. 235.
4. *Kouveliotou C., Strohmayer T., Hurley K. et al.* Discovery of a Magnetar Associated with the Soft Gamma Repeater SGR 1900+14 // *Astrophys. J. Lett.* - 1999. - Vol. 510. - P. L115.
5. *Gotthelf E.V., Vasisht G., Dotani T.* On the Spin History of the X-Ray Pulsar in Kes 73: Further Evidence for an Ultramagnetized Neutron Star // *Astrophys. J. Lett.* - 1999. - Vol. 522. - P. L49.
6. *Kaspi V.M., Chakrabarty D., Steinberger J.* Precision Timing of Two Anomalous X-Ray Pulsars // *Astrophys. J. Lett.* - 1999. - Vol. 525. - P. L33.
7. *Ardeljan N.V., Bisnovatyj-Kogan G.S., Moiseenko S.G.* Magnetorotational supernovae // *MNRAS*. - 2005. - Vol. 359. - P. 333.
8. *Tatsumi T.* Ferromagnetism of quark liquid // *Phys. Lett. B*. - 2000. - Vol. 489. - P. 280.
9. *Galloway D.J., Proctor M.R., Weiss N.O.* Formation of intense magnetic fields near the surface of the sun // *Nature (London)*. - 1977. - Vol. 266. - P. 686.
10. *Feroci M., Hurley K., Duncan R.C., Thompson C.* The Giant Flare of 1998 August 27 from SGR 1900+14. I. An Interpretive Study of BeppoSAX and Ulysses Observations // *Astrophys. J.* - 2001. - V. 549. - P. 1021.
11. *Kondratyev V.N.* Statistics of Magnetic Noise in Neutron Star Crusts // *Phys. Rev. Lett.* - 2002. - Vol. 88. - P. 221101; Magnetization of Neutron Star Matter and Implications in Physics of Soft Gamma Repeaters // *JAERI-Res.* - 2001-057. 75 PP.
12. *Zhang B., Xu R.X., Qiao G.J.* Nature and Nurture: a Model for Soft Gamma-Ray Repeaters // *Astrophys. J.* - 2000. - Vol. 545. - P. L127.
13. *Usov V.V.* Strange Star Heating Events as a Model for Giant Flares of Soft-Gamma-Ray Repeaters // *Phys. Rev. Lett.* - 2001. - Vol. 87. - P. 021101.
14. *Suh I.S., Mathews G.J.* Cold Ideal Equation of State for Strongly Magnetized Neutron Star Matter: Effects on Muon Production and Pion Condensation // *Astrophys. J.* - 2001. - Vol. 546. - P. 1126.
15. *Feynman R.P.* The Feynman lectures on Physics. - London: Addison-Wesley, 1965.
16. *Kondratyev V.N.* Magnetic Shift of Magic Nuclei. *J. Nucl. Sci. Technol.* -2002. - Vol. 1, Suppl. 2. - P. 550; Structure of Nuclei in Strong Magnetic Fields // *J. of Nucl. and Radiochem. Sci.* - 2002. - Vol. 3. - P. 205.
17. *Kondratyev V.N.* Neutron Capture Reactions in Strong Magnetic Fields of Magnetars // *Phys. Rev. C*. - 2004. - Vol. 69. - P. 038801; Nuclear Reactions in Ultra-Magnetized Supernovae // *JAERI-Res.* - 2002-10.
18. *Kondratyev V.N., Kadenko I.M.* Nucleosynthesis in strong magnetic fields at statistical equilibrium // *MNRAS*. 2005. - Vol. 359. - P. 927.
19. *Kondratyev V.N., Kadenko I.M.* Nuclear composition and transmutations of nuclides in ultramagnetized astrophysical plasmas // 55 Int.Workshop on Spectroscopy and Structure of At. Nuclei, Abstracts (Sanct-Petersburg, Russia 2005) and *Bull. RAS* (in press).
20. *Kondratyev V.N., Lutz H.O.* Shell effect in exchange coupling of transition metal dots and their arrays. -*Phys. Rev. Lett.* - 1998. - Vol. 81. - P. 4508.
21. *Kondratyev V.N., Lutz H.O.* Interdot Exchange Coupling in Superferromagnetism // *Eur. Phys. J. D*. - 1999. - Vol. 9. - P. 483.
22. *Kondratyev V.N.* Mean versus strongest signals for self-organized criticality in magnetic quantum dot arrays // *Phys. Lett. A*. - 2006. - Vol. 354. - P. 217 - 220.
23. *Kondratyev V.N., Kadenko I.M., Blanchard Ph.* Arrays of magnetized quantum dots at critical conditions // *J. Mol. Liq.* - 2006. - Vol. 127. - P. 148 - 150.
24. *Hurley K., B. McBreen B., Rabbette M., Steel S.* The lognormal properties of the soft gamma-ray repeater SGR 1806-20 and the VELA pulsar // *AAP*. - 1994. - Vol. 288. - P. L49.
25. *Gogus Ersin et al.* Statistical Properties of SGR 1900+14 Bursts // *Astrophys. J. Lett.* - 1999. - Vol. 526. - P. L93.
26. *Gogus Ersin et al.* Statistical Properties of SGR 1806-20 Bursts // *Astrophys. J. Lett.* - 2000. - Vol. 532. - P. L121.
27. *Ring P., Schuck P.* The Nuclear Many-Body Problem. - Berlin: Springer, 1980.
28. *Kondratyev V.N., Parobiy I.S.* Ionization of atoms at resonant neutron scattering // *Bull. AS USSR*. - 1991. - Vol. 55. - P. 106.
29. *Kondratyev V.N.* Anomalous Reduction of beta-decay Rate due to Resonant Energy Absorption // *Z. Phys. B*. - 1996. - Vol. 99. - P. 473.

МАГНИТОДИНАМИКА МАГИЧЕСКИХ ЯДЕР В КОРЕ МАГНИТАРОВ

В. Н. Кондратьев, И. Н. Каденко

Рассмотрена магнитодинамика неоднородной ядерной материи, соответствующей коре нейтронных звезд. Продемонстрировано, что эффекты квантования приводят к резким скачкообразным аномалиям в зависимости магнитных моментов нуклидов от магнитного поля. Учитывая магнитное взаимодействие между нуклидами, мы показываем, что такие аномалии приводят к разрывообразным скачкам в магнитодинамике коры нейтронных звезд. Свойства таких шумов удовлетворительно согласуются со статистикой активности источников мягких повторяющихся гамма-всплесков.

МАГНИТОДИНАМІКА МАГІЧНИХ ЯДЕР У КОРІ МАГНІТАРІВ

В. М. Кондратьєв, І. М. Каденко

Розглянуто магнітодинаміку неоднорідної ядерної матерії, що відповідає корі нейтронних зірок. Продемонстровано, що ефекти квантування приводять до різких стрибкоподібних аномалій у залежності магнітних моментів нуклідів від магнітного поля. З огляду на магнітну взаємодію між нуклідами ми показуємо, що такі аномалії приводять до розривоподібних стрибків у магнітній динаміці корі нейтронних зірок. Властивості таких шумів задовільно узгоджуються зі статистикою активності джерел м'яких повторюваних гамма-сплесків.